31st Annual International Conference of the IEEE EMBS
Minneapolis, Minnesota, USA, September 2-6, 2009

An automated quantification of the transmural myocardial infarct extent using cardiac DE-MR images

R. El Berbari, N. Kachenoura, F. Frouin, A. Herment, E. Mousseaux, and I. Bloch

Abstract— **Evaluating myocardial viability is an important prognostic factor in the follow-up of infarctions. Delayed Enhancement magnetic resonance (DE-MR) imaging allows precise delineation of the infarct transmural extent. Visual interpretation is the most commonly used method to assess the myocardial infarction (MI) transmural extent. This study proposes to automate the segmentation of the (DE) images prior to the estimation of the extent of infarcted tissue. Indeed the segmentation of the myocardium was performed using cine contraction images which present a high contrast between cavity and myocardium. After the segmentation, the segmental transmurality is estimated on a conventional five point scale. A head to head comparison was performed between visual and quantitative analysis of infarct transmurality on DE-MR imaging. Results on 921 sub-segments (9 patients) showed an absolute agreement of 80% and a relative agreement (with one point difference) of 97%.**

I. INTRODUCTION

The extent and degree of myocardial injury after an acute ischemic event are strong predictors of patient outcome, and can be used to determine whether regions of abnormal ventricular contraction will improve after revascularization in patients with coronary artery disease. Indeed, the functional recovery is inversely correlated to the extent of the myocardial infarct [1]. Studies [2] have shown that revascularization can improve the contractile function of an affected segment when the transmural extent is less than 50% of the total myocardial thickness.

Noninvasive methods for assessing myocardial viability include positron- emission tomography (PET) and single-photon-emission computed tomography (SPECT). These techniques have proven clinical utility, but each has limitations that may reduce its diagnostic accuracy. For example, they interpret myocardial viability as an all-or-nothing phenomenon within a myocardial region, since none of them can assess the transmural extent of viability of the ventricular wall.

Delayed Enhancement Magnetic Resonance (DE-MR) imaging offers high spatial resolution images that can be used to identify acute myocardial infarction and to distinguish between reversible and irreversible myocardial ischemic injury.

R. El Berbari is with INSERM U678, UPMC, F-75013 Paris France and Téécom ParisTech (ENST), CNRS UMR 5141, F-75013 Paris France relberba@imed.jussieu.fr Tel: (+33) 153828423 Fax: (+33) 153828448

I. Bloch is with Téécom ParisTech (ENST), CNRS UMR 5141, F-75013 Paris France

E. Mousseaux is with APHP, HEGP Department of Cardiovascular Radiology, F-75015 Paris France and INSERM U678 UPMC, F-75013 Paris France

N. Kachenoura, A. Herment and F. Frouin are with INSERM U678, UPMC, F-75013 Paris France

Available results suggest that the myocardial infarcted volume detected using DE-MR imaging is well correlated with that measured using PET [3] and this technique allows visualization of transmural and subendocardial myocardial infarcts that can be missed by SPECT [4], [5].

Nowadays, DE-MR acquisition is considered to be the method of choice for assessing myocardial infarct volume. In clinical routine, DE images are interpreted visually [6]. However a precise quantification of the infarct size would be necessary to achieve a better follow-up of patients. That the reason why different algorithms were proposed for quantifying infarcted zones. However, differentiating between the left ventricle cavity and the infarcted area in a DE image involves a major difficulty, owing to the fact that blood and infarcted zone have almost the same grey level intensity. So in the majority of studies, endocardial and epicardial contours were outlined manually and different algorithms were then applied for quantifying infarcted zones [7], [8], [9], [10].

A limited number of studies proposed an automated or semi-automated segmentation of the myocardium in DE images [11], [12], [13], [14].

In this paper, we suggest a method to segment the myocardium on DE images using the contraction (cine) images because of their high contrast between cavity and myocardium and then to quantify the myocardial infarct extent and provide segmental transmurality scores on patients with myocardial infarction. In Section 2 the main steps of the segmentation method and the quantification process are described. Results of the estimated segmental transmurality scores are presented and compared with visual scores in Section 3 and are finally discussed in Section 4.

II. MATERIAL AND METHOD

A. Population and acquisition protocol

Nine patients with myocardial infarction were prospectively studied. MR acquisitions, including a dynamic study of the contraction (cine images) and a static study of the DE, were acquired at the European Hospital Georges Pompidou. All studies were performed according to a standard protocol on a 1.5-T MRI system (Signa LX, GE Medical Systems, Milwaukee, WI) with an 8-element thoracic phased-array surface coil. This protocol was done as follows: Contraction cine loops with ECG gating were obtained using Fast Imaging Employing Steady State Acquisition (FIESTA), a steady state free precession (SSFP) technique with the following acquisition parameters: repetition time: $3.7-4$ ms; echo time: $1.6-1.7$ ms; flip angle: 50 degree; slice thickness: 8 mm; inter slice gap: 1 mm; pixel size: 0.7x0.7 - 1.7x$1.7 mm^2$.

978-1-4244-3296-7/09/$25.00 ©2009 IEEE

After that, a contrast agent (Gd-DTPA) was injected to the patient and 10 to 15 minutes after the injection 3D-Delayed Enhancement images were acquired with the following parameters: repetition time: $4.3 - 5.5$ ms; echo time: $1 - 2$ ms; flip angle: 15 degree; slice thickness: 6 mm; pixel size: 1.4x1.4 - 1.5x1.5mm^2; inversion time: 150 - 200 ms and trigger delay: 300 ms, and space between slices: 3 mm .

All MR images were acquired using breath-holding. Cine loops were acquired in 12 to 14 short-axis views from the mitral annulus to the apex. DE images in 24 to 32 short-axis views from the mitral annulus to the apex.

B. Reference scoring of segmental MI transmural extent

To define an adequate segmentation of the myocardium in each short-axis view, two points including the left ventricle center P_0 and the anterior intersection between the right and left ventricles P_1, were defined by the operator. Using P_0 and P_1), a region of interest (ROI) was then defined [15] and six angular sectors were automatically drawn according to the recommended standardized LV model [16] as: anterior (A), anterolateral (AL), inferolateral (IL), inferior (I), inferoseptal (IS), and anteroseptal (AS) segments. Each sector was further subdivided into 3 sub-segments to take into account the heterogeneity of the delayed enhancement in each segment [10]. For all patients, sub-segments transmural extent were assessed by an expert according to a five-point scale (0: no infarction; 1: transmurality $< 25\%$; 2: transmurality from 26% to 50%; 3: transmurality from 51% to 75%; 4: transmurality from 76% to 100%).

C. Method

The proposed method relied on the following principles: the myocardium was automatically delineated using cine images because of their high contrast between cavity and muscle and the resulting contours were registered and superimposed on DE images prior to the estimation of the extent of infarcted tissue.

1) Temporal and spatial registration: First, a temporal registration between the two data sets, Cine and DE, was performed in order to compute a synthetic image of contraction that best corresponded to the DE image. The synchronization of the two studies with the ECG was used to define the temporal zone *Z* through the cardiac cycle corresponding to the DE acquisition. The DE image acquisition time lasts up to four or five times the cine image acquisition time (Figure 1). In order to obtain the best temporal correspondence between both cine and DE sets for each slice an average cine image was calculated by summing all cine images that were acquired during temporal zone *Z*. Thus cine set was temporally registered to the DE set.

In a second phase, a spatial registration based on a 3D scaling followed by a rigid 3D transformation was performed in order to position the two data sets toward the same machine reference. Specific parameters related to the patient orientation and the voxel dimensions were extracted from the original DICOM data format in order to adjust automatically scale and orientation differences.

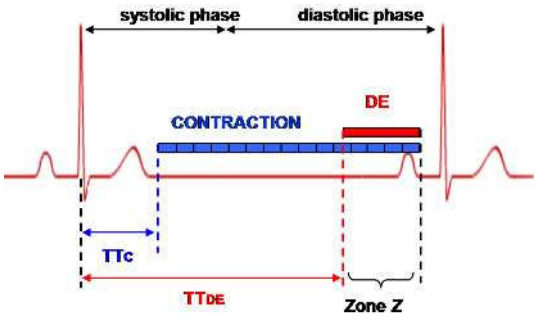

Fig. 1. Temporal registration using the synchronization of the two studies with the ECG.

2) Myocardial segmentation on cine images: An automated segmentation method [17], [18] robust to the presence of the papillary muscles and the poor homogeneity of the left cavity was applied to cine images in order to obtain an accurate endocardial contour. The method consisted in a filtering step applied to the original image using connected filters, followed by the GVF snake algorithm. An optimal choice of the size parameter λ of the filter was done as described in [17], [18].

A first contour was defined on the filtered images using P_0 as an initialization and the GVF snake method with the following parameters: $\alpha = 1$, $\beta = 40$ (defining the regularity of the contour), $\kappa = 1.6$ (weight of the pressure force), $\kappa_p = 0.6$ and $\mu_{gvf} = 0.3$ (parameters defining the diffused gradient force). The high value of β generated a rigid contour enclosing the papillary muscles into the cavity. A refinement of this segmentation was necessary in order to recover boundary information and catch all details that might be lost during the filtering process. Thus, the first contour was used as initialization of a new segmentation, applied to the gradient of the original image with lower values of $\beta = 10$, $\kappa_p = 0.3$ and $\mu_{gvf} = 0.1$. This segmentation method was validated on control subjects and patients [18], [17].

The epicardial border was detected using the GVF snake initialized by an ellipse fitted to eight points clicked into the myocardium. GVF snake parameters were settled as follows: $\alpha = 1$, $\beta = 50$, $\kappa = 1.8$, $\kappa_p = 0.1$ and $\mu_{gvf} = 0.3$.

3) Myocardial segmentation on DE images: A final registration was applied to take into account a possible shift between cine and DE studies. A cine contour volume was obtained by stacking for all processed slice levels binary images containing both endocardial and epicardial contours. On the other hand, a binary DE gradient volume was obtained from the 2D spatial gradient intensity of DE images. A 2D rigid registration based on a shift window of dimension [a_x, a_y],[b_x, b_y] in both the vertical and horizontal directions was applied to each pair matching DE gradient image and cine contour image, testing all possible combinations of integer shift. A superposition index I was defined as follows:

$$I = k_1 N_1 + k_2 N_2 + k_3 N_3 \quad (1)$$

where N_1 was the number of pixels which superposed exactly between the cine contour image and the DE gradient

image, N_2 the number of pixels which superposed according to a four connectivity criterion (i.e. superposition with one of the four neighbors of the contour points), and N_3 the number of pixels which superposed according to an eight connectivity criterion. Weighting coefficients were fixed as ($k_1 = 1$, $k_2 = \frac{1}{4}$, $k_3 = \frac{1}{8}$). The shift window bounds were fixed as $[-2, +2][-2, +2]$. The optimal transformation was obtained using registration parameters that gave the best correspondence between the DE gradient volume and the cine contour volume.

4) Transmural extent scoring: As described in [10] a fuzzy c-means algorithm was used to classify pixels into enhanced pixels C_E class and non enhanced pixels C_{NE} class. A membership function to the enhanced class was calculated for all myocardial pixels. The previously described sub-segments were circumferentially divided into four layers: L_k ($k = 1, ..., 4$). Then for each angular region defined by a sub-segment S_j ($j = 1, ..., 18$) and a layer L_k, an index of DE extension $N_{j,k}$, was computed as the mean membership degree to the (C_E) class [10]. This decomposition was done in order to integrate the fact that the infarct spreads in a wave-front extension from the endocardium to the epicardium.
Moreover, three modifications were proposed.

- A modified fuzzy c-means algorithm is used, such that pixels with a grey level less then the center of the C_{NE} class have a membership degree to this class equal to 1 and a membership to the C_E class equal to 0 and vice-versa for pixels with a grey level higher than the center of the C_E class. This ensures the monotony of the membership functions with respect to the distance to the class center.
- In order to take into account slice levels where all sectors were completely enhanced, the 2D clustering was replaced by a 3D clustering when the relative ratio between the grey levels of the two centers of class was to low.
- For each angular region, the infarct transmurality scores were assessed using an hysteresis threshold, Th_1 being the lower value and Th_2 the upper value, instead of one single threshold. Let $N_{j,k}$, be the index of extension in the sub-segment S_j and the layer L_k,score was initialized to 0 and successively updated as follows:
  - if $N_{j,1} > Th_2$, then score =1,
  - if $N_{j,1} > Th_1$ and $N_{j,2} > Th_2$, then score =2,
  - if $N_{j,1} > Th_1$ and $N_{j,2} > Th_1$ and $N_{j,3} > Th_2$, then score =3,
  - if $N_{j,1} > Th_1$ and $N_{j,2} > Th_1$ and $N_{j,3} > Th_1$ and $N_{j,4} > Th_2$, then score =4.

Th_1 and Th_2 were chosen equal to 0.30 and 0.45.

III. RESULTS

Figure 2 depicts, for each slice level, the segmentation results on both cine and DE images. A total of 921 sub-segments were analyzed (15 angular subsegments showing a no reflow pattern were excluded from the visual analysis).

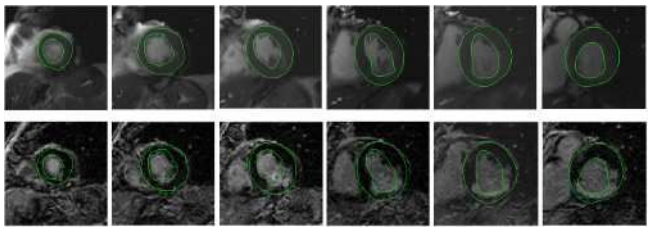

Fig. 2. Contours provided by the automatic segmentation, for different slice levels from the apex (top left) to the base (bottom right) on both cine images (first row) and their superimposition after registration on DE images (second raw).

A head-to-head comparison was performed between the visual classification, made by an expert and the proposed method on the 921 sub-segments of the database. An absolute agreement (segments were categorized similarly by visual and quantitative analysis) of 80% was found, and a relative agreement (a difference of one, respectively two, between the quantitative scores and the expert scores was accepted) of 97% (respectively 99%) were obtained. The excellent agreement was estimated by a value of 0.815 for the weighted Kappa coefficient.

Table I presents the contingency table of comparison between visual assessment and the proposed method.

		Visual				
		0	**1**	**2**	**3**	**4**
Quantitative	**0**	584	13	9	2	1
	1	40	24	12		1
	2	4	12	47	35	6
	3	2		7	13	40
	4				2	67

TABLE I

COMPARISON OF TRANSMURAL EXTENT SCORES BETWEEN EXPERT AND COMPUTER-ASSISTED METHOD IN THE 921 ANGULAR SUB-SEGMENTS OF THE DATABASE.

IV. DISCUSSION AND CONCLUSION

This paper addressed the task of automating the delineation of the myocardium of delayed enhancement images using the corresponding cine anatomical sequences.

The proposed method is validated using visual inspection as a gold standard. Very encouraging results were obtained by our method (80% of absolute agreement and $\kappa = 0.815$) to be compared with [19] (absolute agreement of 90% and $\kappa = 0.86$) and [10] (absolute agreement of 88% and $\kappa = 0.86$), for which contours were manually delineated in both cases.

Among 921 sub-segments analyzed, six heavy misclassifications were highlighted (with a score difference greater than 2 between visual and quantitative scores). Among these 6 errors, 3 were due to an artifact on the native images. Other errors were due to an irregularity in the shape of the infarcted area: the first layer appeared as non-enhanced, whereas the second and third layers were strongly enhanced; moreover, the neighboring sub-segment was fully enhanced. Quantitative method assigns a low score to such sub-segments, while

the visual score was higher. These sub-segments could have been better classified by introducing continuity rules between adjacent sub-segments.

Some sub-segments have an enhancement index close to the used thresholds, they can be considered as borderline cases and present slight difference between visual and quantitative scoring.

In general, transmural extent was under-estimated by the algorithm, when compared to the expert reading. One possible explanation is that the expert could slightly overestimate the transmurality extent of the infarct, especially when it is large. Indeed, the distinction between two classes was difficult to establish visually for some intermediate cases such as score 2 ($< 50\%$) and score 3 ($> 51\%$).

The effect of the cavity border was also tested by an outward expansion of the endocardial contour by one pixel before applying the quantitative process. Comparing to the visual scores, for this new contour, the absolute agreement was 79%, and $\kappa = 0.803$. Using dilated contour, the number of normal sub-segments that were affected by the score 1 has decreased, thus a further investigation is needed. Nevertheless, an excellent concordance between quantitative scores estimated using the original endocardial contour and its morphological dilation by one pixel were shown with an absolute agreement of 92% and a weighted Kappa coefficient of 0.932. This proves the robustness of the method against the endocardial segmentation with a variability of one pixel.

In conclusion, the proposed method could stand as a valuable tool to automatically segment DE images and accurately assess segmental infarct transmurality. However, the evaluation must be extended to a larger series of patients. Besides combining segmental transmurality estimation with segmental assessment of myocardial wall motion from cine images [15] could help identifying wall motion abnormalities and myocardial viability in clinical studies.

REFERENCES

[1] Selvanayagam, J.B. and Kardos, A. and Francis, J.M. and Wiesmann, F. and Petersen, S.E. and Taggart, D.P. and Neubauer, S., " Value of delayed-enhancement cardiovascular magnetic resonance imaging in predicting myocardial viability after surgical revascularization ", *Circulation*, vol. 110, 2004, pp. 1535-1541.

[2] Mollet, N.R. and Dymarkowski, S. and Volders, W. and Wathiong, J. and Herbots, L. and Rademakers, F.E. and Bogaert, J., "Visualization of ventricular thrombi with Contrast Enhanced Magnetic Resonance Imaging in patients with ischemic heart disease", *Circulation*, vol. 106, 2002, pp. 2873-2876.

[3] Klein, C. and Nekolla, S.G. and Bengel, F.M. and Momose, M. and Sammer, A. and Haas, F. and Schnackenburg, B. and Delius, W. and Mudra, H. and Wolfram, D. and Schwaiger, M., "Assessment of myocardial viability with contrast-enhenced Magnetic Resonnance Imaging: Comparison with Positron Emission Tomography", *Circulation*, vol. 105, 2002, pp. 162-167.

[4] Wagner, A. and Mahrholdt, H. and Holly, T.A. and Elliott, M.D. and Regenfus, M. and Parker, M. Klocke, F.J. and Bonow, R.O. and Kim, R.J. and Judd, R.M., "Contrast-enhanced MRI and routine single photon emission computed tomography (SPECT) perfusion imaging for detection of subendocardial myocardial infarcts: an imaging study", *Lancet*, vol. 361, 2003, pp. 374-379.

[5] Kuhl, H.P. and Beek, A.M. and Van der Weerdt, A.P. and Hofman, M.B.M. and Visser, C.A. and Lammertsma, A.A. and Heussen, N. and Visser, F.C. and Van Rossum, A.C., "Myocardial viability in chronic ischemic heart disease : comparison of contrast-enhanced Magnetic Resonance Imaging with (18) F-fluorodeoxyglucose Positron Emission Tomography", *Journal of the American College of Cardiology*, vol. 41, 2003, pp. 1341-1348.

[6] Comte, A. and Lalande, A. and Walker, P.M. and Cochet, A. and Legrand, L. and Cottin, Y. and Wolf, J.E. and Brunotte, F., "Visual estimation of the global myocardial extent of hyperenhancement on delayed contrast-enhanced MRI", *European Radiology*, vol. 14, 2004, pp. 2182-2187.

[7] Kolipaka, A. and Chatzimavroudis, G.P. and White, R.D. and ODonnell, T.P. and Setser, R.M., "Segmentation of non-viable myocardium in delayed enhancement magnetic resonance images", *The International Journal of Cardiovascular Imaging* vol. 21, 2005, pp.303-311.

[8] Hsu, L.Y. and Ingkanisorn, W.P. and Kellman, P. and Aletras, A.H. and Arai, A.E., "Quantitative myocardial infarction on delayed enhancement MRI. Part II: clinical application of an automated feature analysis and combined thresholding infarct sizing algorithm", *Journal of Magnetic Resonance Imaging*, vol. 23, 2006, pp. 309-314.

[9] Rosendahl, L. and Blomstrand, P. and Heiberg, E. and Ohlsson, J. and Bjrklund, P.G. and Ahlander, B.M. and Engvall, J., "Computer-assisted calculation of myocardial infarct size shortens the evaluation time of contrast-enhanced cardiac MRI", *Clinical Physiology and Functional Imaging*, vol. 28, 2008, pp. 1-7.

[10] Kachenoura, N. and Redheuil, A. and Herment, A. and Mousseaux, E. and Frouin, F., "Robust assessment of the transmural extent of myocardial infarction in late gadolinium-enhanced MRI studies using appropriate angular and circumferential subdivision of the myocardium", *European Radiology*, vol. 18, 2008, pp. 2140-2147.

[11] Positano, V. and Pingitore, A. and Giorgetti, A. and Favilli, B. and Santarelli, M.F. and Landini, L. and Marzullo, P. and Lombardi, M., "A fast and effective method to assess myocardial necrosis by means of contrast magnetic resonance imaging", *Journal of Cardiovascular Magnetic Resonance*, vol. 7, 2005, pp. 487-494.

[12] Noble, N.M.I. and Hill, D.L.G. and Breeuwer, M. and Razavi, R., "The automatic identification of hibernating myocardium", *Medical Image Computing and Computer Assisted Intervention (MICCAI)*, LNCS, France, vol. 3217, 2004, pp. 890-898.

[13] Dikici, E. and O'Donnell, T. and Setser, R. and White, R.D., "Quantification of Delayed Enhancement MR Images", *Medical Image Computing and Computer Assisted Intervention (MICCAI)*, LNCS, France, vol. 3216, 2004, pp. 250-257.

[14] Ciofolo, C. and Fradkin, M. and Mory, B. and Hautvast, G. and Breeuwer, M., "Automatic myocardium segmentation in late-enhancement MRI", *IEEE International Symposium on Biomedical Imaging: From Nano to Macro*, 2008, pp. 225-228.

[15] El Berbari, R. and Kachenoura, N. and Redheuil, A. and Giron, A. and Mousseaux, E. and Herment, A. and Bloch, I. and Frouin, F., "An Automated Estimation of Regional Mean Transition Times and Radial Velocities from Cine Magnetic Resonance Images. Evaluation in Normal Subjects", *Journal of Magnetic Resonance Imaging*, 2009, in press.

[16] Cerqueira, M.D. and Weissman, N.J. and Dilsizian, V. and Jacobs, A.K. and Kaul, S. and Laskey, W.K. and Pennell, D.J. and Rumberger, J.A. and Ryan, T. and Verani, M.S., "Standardized myocardial segmentation and nomenclature for tomographic imaging of the heart: a statement for healthcare professionals from the Cardiac Imaging Committee of the Council on Clinical Cardiology of the American Heart Association", *Circulation*, vol. 105, 2002, pp. 539-542.

[17] El Berbari, R. and Frouin, F. and Redheuil, A.B. and Angelini, E.D. and Mousseaux, E. and Bloch, I. and Herment, A., "Dveloppement et valuation d'une mthode de segmentation automatique de l'endocarde sur des images acquises par rsonance magntique", *ITBM-RBM*, vol. 28, 2007, pp. 117-123.

[18] El Berbari, R. and Bloch, I. and Redheuil, A.B. and Angelini, E.D. and Mousseaux, E. and Frouin, F. and Herment, A., "Automated segmentation of the left ventricle including papillary muscles in Cardiac Magnetic Resonance images", *Fourth International Conference on Functional Imaging and Modeling of the Heart (FIMH)*, Salt Lake City, Utah, USA, vol. 4466, 2007, pp. 453-462.

[19] Schuijf, J.D. and Kaandorp, T.A.M. and Lamb, H.J. and van der Geest, R.J. and Viergever, E.P.and van der Wall, E.E. and de Roos, A. and Bax, J.J., "Quantification of Myocardial Infarct Size and Transmurality by Contrast-Enhanced Magnetic Resonance Imaging in Men", *Am J Cardiol*, vol. 94, 2004, pp. 284288.